Geometrodynamic Probes in Light Theory Realm Curvature, Information Density, and Reeb Flow in Prime-Plaquette Models

Dimitry Jean-Noel II
Pleroma Works, LLC
djean@botwpbc.com
Secondary: djeannoelii@gmail.com
ORCID: 0009-0009-6082-8647

Version 0.1.0 (experiments)

Abstract

Light Theory Realm implements a geometrodynamical framework where the fundamental object is the geometry of information: a Quantum Geometric Tensor (QGT) defined on a parameter manifold of states. The theory papers *Foundations of Light Theory* and *Light Mechanics* develop the conceptual and mathematical structure: Clifford algebra $Cl(1,3)$, QGT-based information metrics, Kaluza–Klein uplift, contact geometry, Reeb flow, and an information-geometric equation of state (IGBP).

This paper presents the first experimental results obtained with the public Light Theory Realm implementation. We report:

1. A prime-plaquette scan over nine Standard Model fermions, recording information-geometric densities and convergence behaviour of the IGBP flow.
2. A curvature burst analysis using an exponential parameterisation of the geometrodynamical flow, yielding per-particle curvature bursts $R_{\max}$ across leptons and quarks.
3. A gravity-probe parameter scan over a two-dimensional family of loops in parameter space, mapping the joint behaviour of Fisher metric norm, Berry curvature norm, information-geometric density ρ_{IGBP}, and a Reeb-flow norm.

The results show that (i) Berry curvature and Fisher metric norms are strongly correlated across the scanned parameter space, (ii) the IGBP density is anti-correlated with both metric and curvature norms but positively correlated with Reeb-flow strength, and (iii) information-geometric densities associated with prime plaquettes span several orders of magnitude before relaxation but show no simple monotone relation with particle mass at this stage. We close by outlining how these probes can be extended into systematic tests of Light Theory's geometrodynamical and holographic claims.

1 Introduction

Light Theory treats physical and learning systems as curved manifolds of information. A family of states $|\psi(\theta)\rangle$, depending on parameters θ^u, carries a QGT $Q_{uv}(\theta)$ whose real part defines a Fisher metric g_{uv} and whose imaginary part defines a Berry curvature Ω_{uv}.

In *Light Mechanics*, this information geometry is promoted to a geometrodynamical field theory: an Einstein–Fisher-like relation ties information fluctuations to curvature; a 5D Kaluza–Klein uplift builds a bulk metric from (g_{uv}, A_u); a contact structure and Reeb vector encode intrinsic time; and the IGBP equation of state ρ_{IGBP} compares gradients of a representative entropy S_{rep} with curvature invariants.

The present work asks what this geometry looks like for concrete, finite-dimensional models and how it relates to the prime plaquette structure used to mimic Standard Model fermions. We focus on three experimental pipelines: (1) prime-plaquette scans over nine fermions; (2) next-generation curvature bursts under exponential geometrodynamical flow; and (3) a gravity probe sweeping a two-dimensional parameter family of loops. All experiments use the public Light Theory Realm codebase and are reproducible from the CSVs and plotting scripts included in the repository.

2 Experimental setup

2.1 Geometry engine

All experiments use the same geometric backbone (fully described in *Light Mechanics*):

- A `CliffordEngine` implementing $Cl(1,3)$ gamma matrices, grade projection, and wedge products.
- A `CliffordQGT` module that, given a state $\psi(\theta)$ and its Jacobian $J = \partial\psi/\partial\theta$, computes the full QGT and returns the Fisher information metric g_{uv} and Berry curvature Ω_{uv}.

Derived scalars include: (i) `fisher_norm`, the Frobenius norm $\|g\|_F$; (ii) `berry_norm`, the Frobenius norm $\|\Omega\|_F$; (iii) `rho_igbp`, the information-geometric density; and (iv) `reeb_norm`, the norm of the Reeb vector field with respect to the information metric.

2.2 Prime plaquettes and particle assignments

Prime plaquettes are short ordered lists of distinct primes, e.g.

$$
\begin{aligned}
e^- &\leftrightarrow [2,3,5,7],\\
\mu^- &\leftrightarrow [2,17,23,7],\\
\tau^- &\leftrightarrow [3,11,13,47],
\end{aligned}
$$

for the nine charged Standard Model fermions. Each plaquette defines a discretised loop $\mathcal{C}$ in parameter space and a corresponding Wilson-loop-like observable built from the Berry connection. Initial conditions $\phi_{\mathrm{initial}}, \omega_{\mathrm{initial}}$, and $\rho_{\mathrm{IGBP,initial}}$ are set per plaquette.

The prime-plaquette dataset [5] and joined analysis table [4] record, per particle: physical mass m_{phys} (MeV), plaquette assignment, initial and final IGBP densities, a scalar entropy S_{rep}

after relaxation, curvature metrics (currently vanishing in this pipeline), and log-transformed quantities for analysis.

2.3 Next-generation curvature bursts

Earlier curvature extraction produced vanishing curvature scalars R for these plaquettes, as recorded in [1]. To probe beyond this limitation we implemented an exponential geometrodynamical flow: the state is evolved using a flow operator derived from the sixth-order master information operator L_6, and curvature scalars are monitored along the flow.

The resulting dataset [3] contains, for each particle: m_{phys}, $R_{\max}$, $|R|_{\max}$, `burst_time`, and `n_samples` used along the flow.

2.4 Gravity probe: two-dimensional parameter scan

The gravity probe is a dense scan over a two-dimensional parameter family of loops:

- Loop scale $s \in [0.1, 2.0]$,
- Rotation angle $\alpha_1 \in [0, \pi]$,
- Second rotation angle fixed at $\alpha_2 = \pi/4$,
- Reeb-coupling parameter $\xi_{\text{res}} = 1/7$.

We sample 20 evenly spaced values of s and 20 values of α_1 for a total of 400 configurations. For each configuration we compute `fisher_norm`, `berry_norm`, `rho_igbp`, and `reeb_norm`. Results are stored in [2] and visualised as heatmaps for the Berry curvature norm, Fisher metric norm, and ρ_{IGBP}.

3 Results

3.1 Prime plaquette IGBP and convergence

The prime-plaquette scan shows that initial IGBP densities span roughly an order of magnitude across plaquettes, with $\log_{10} \rho_{\text{IGBP,initial}} \approx 8.4$–$8.8$. All plaquettes in this run relax to $\rho_{\text{IGBP,final}} = 0$ under the current flow, requiring two to three convergence steps for the leptons and two steps for several quarks.

The joined analysis [4] shows a small, negative correlation between log mass and log initial IGBP density,

$$\text{corr}(\log m, \log \rho_{\text{init}}) \approx -0.49,$$

on this nine-point dataset. Given the tiny sample size and limited dynamic range, this should be interpreted as no clear monotone trend rather than evidence of an inverse law. The curvature metrics R_{rms} and $R_{\max}$ are identically zero in this pipeline, confirming that the original curvature extraction was effectively flat for these configurations and motivating the next-generation exponential pipeline.

3.2 Curvature bursts under exponential flow

The next-generation curvature dataset [3] shows large curvature bursts $|R|_{\max} \sim 10^{21}$–10^{25} across all particles, indicating that the exponential flow strongly excites curvature before relaxing. Bursts occur very early in flow time (`burst_time` ≈ 0.0–0.1 in the current units), suggesting that the geometry rings quickly once pushed off the flat initial configuration. A Pearson correlation between mass and $|R|_{\max}$ is small and negative,

$$\mathrm{corr}(m_{\mathrm{phys}}, |R|_{\max}) \approx -0.19,$$

consistent with no simple monotone relationship in the present coarse setup. The current exponential flow parameterisation is clearly capable of generating substantial curvature excitations, but the mapping from these bursts to physical mass scales is not yet clean and will need regularisation for meaningful cross-plaquette comparisons.

3.3 Gravity probe: Fisher, Berry, and IGBP over (α_1, s)

The 400-point gravity-probe scan reveals several robust patterns.

Global statistics. From [2]:

- ρ_{IGBP}: mean ≈ 4.30, median ≈ 0.53, range 0.004–122.1, strongly right-skewed.
- `fisher_norm`: mean ≈ 1.26, median ≈ 1.32, range 0.64–3.92.
- `berry_norm`: mean ≈ 0.24, median ≈ 0.04, range 8×10^{-4}–1.82.
- `reeb_norm`: mean ≈ 1.65, median ≈ 1.67, range 0.86–2.42.

The configuration with maximum Berry curvature is $s = 0.1$, $\alpha_1 = 0$ with `berry_norm` ≈ 1.82 and `fisher_norm` ≈ 3.92. The configuration with maximum IGBP density is $s = 0.1$, $\alpha_1 = \pi$, with $\rho_{\mathrm{IGBP}} \approx 122.1$, `berry_norm` ≈ 0.0014, `fisher_norm` ≈ 0.64, and `reeb_norm` ≈ 2.33.

Correlations. The correlation matrix over the 400 samples shows:

$$\begin{aligned} \mathrm{corr}(\texttt{fisher\_norm}, \texttt{berry\_norm}) &\approx 0.59, \\ \mathrm{corr}(\rho_{\mathrm{IGBP}}, \texttt{fisher\_norm}) &\approx -0.41, \\ \mathrm{corr}(\rho_{\mathrm{IGBP}}, \texttt{berry\_norm}) &\approx -0.20, \\ \mathrm{corr}(\rho_{\mathrm{IGBP}}, \texttt{reeb\_norm}) &\approx +0.31. \end{aligned}$$

In this experiment, information density spikes not where curvature is largest, but where the Reeb flow is strong and the metric appears soft.

Heatmap structure. The heatmaps make these patterns visually clear:

- Berry curvature norm concentrates at small α_1, especially at small loop scales s. It decays quickly with increasing α_1 and is negligible by $\alpha_1 \gtrsim 1.5$.
- Fisher metric norm is also largest at small α_1 and small s, but decays more slowly, leaving a plateau once s is large.

- ρ_{IGBP} is small where Fisher and Berry norms are maximal, but grows sharply near $\alpha_1 \approx \pi$ at small loop scale $s \approx 0.1$, forming a high-density ridge that coincides with strong Reeb-flow norms but weak metric and curvature norms.

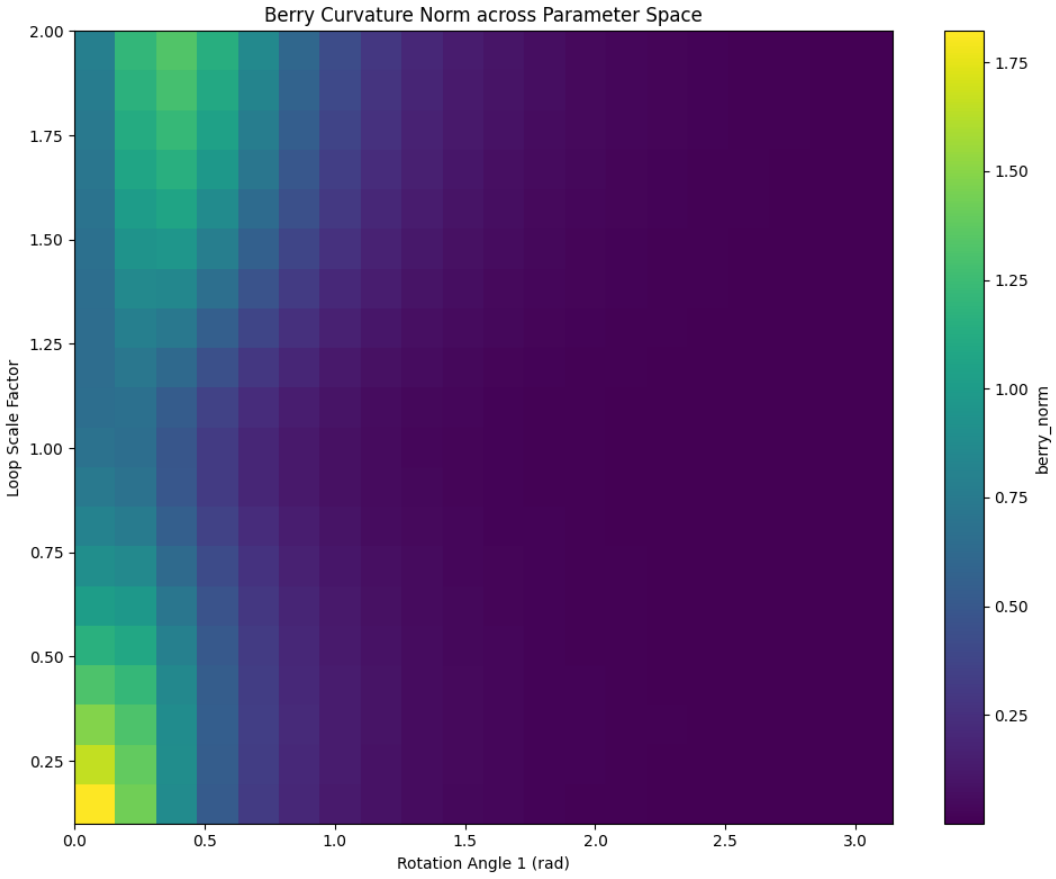

Figure 1: Berry curvature norm heatmap over (α_1, s).

4 Discussion

4.1 Geometrodynamics and the role of the Reeb flow

The gravity-probe correlations line up with the geometrodynamical picture in *Light Mechanics*: the metric g_{uv} and curvature Ω_{uv} encode static local geometry, while the Reeb vector field encodes preferred flow in the contact-geometry sense. The observed pattern—high Fisher and Berry norms where ρ_{IGBP} is small, and high ρ_{IGBP} where metric and curvature norms are low but Reeb flow is strong—is consistent with the idea that information density is driven not just by static curvature, but by how strongly the Reeb flow pumps volume through the geometry. Curvature sets the stage; Reeb flow moves the actors.

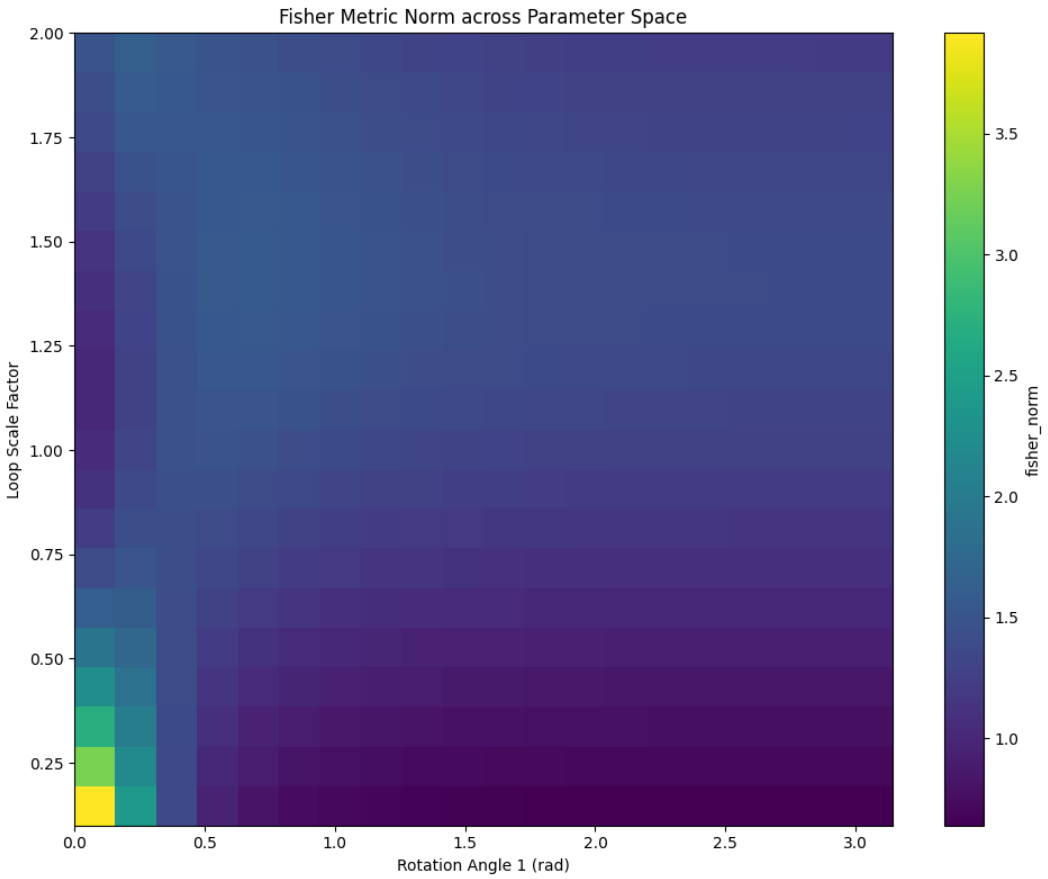

Figure 2: Fisher metric norm heatmap over (α_1, s).

4.2 Limitations of the current pipelines

1. Small sample sizes in the particle sector: nine fermions mean correlations between mass, IGBP, and curvature are qualitative hints, not robust laws.
2. Incomplete curvature regularisation: exponential bursts reach $|R|_{\max} \sim 10^{21}$–10^{25}. Without regularisation, comparing these across plaquettes is delicate.
3. Simplified loop parameterisation: the gravity probe uses a specific two-parameter family of loops. There is no guarantee that these probes explore the most physically relevant directions in parameter space.
4. Model dependence: results depend on plaquette assignments, Reeb coupling ξ_{res}, and the IGBP definition and normalisation.

4.3 Holographic interpretation

From the holographic viewpoint of Light Theory, the gravity-probe experiments live on the boundary information manifold. The QGT data (g_{uv}, Ω_{uv}) and IGBP densities constitute boundary data for a higher-dimensional bulk metric via the Kaluza–Klein uplift. The observed

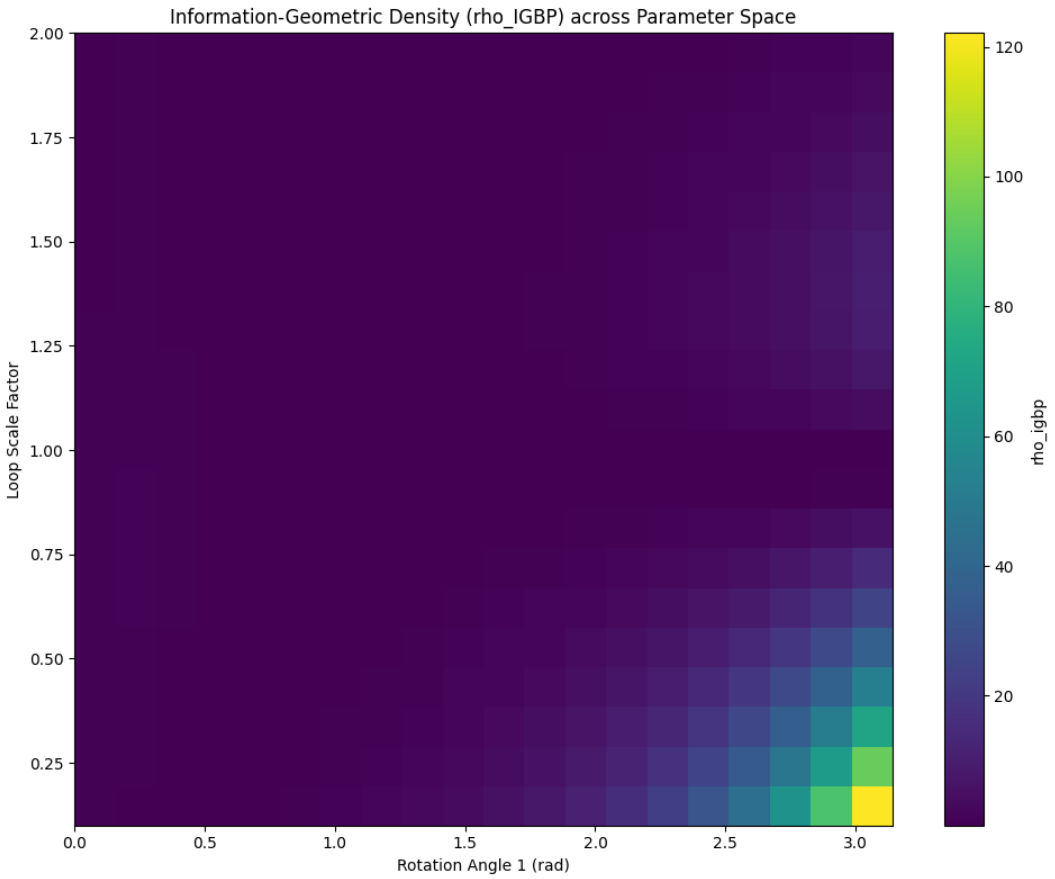

Figure 3: Information-geometric density ρ_{IGBP} over (α_1, s).

concentration of ρ_{IGBP} in specific regions of parameter space hints that the dual bulk geometry may develop localised throats or bubbles corresponding to high-density Reeb flows with relatively mild boundary curvature where these throats attach. A fully worked-out bulk solution is beyond the scope of this paper, but the experimental patterns provide concrete boundary conditions that any bulk geometrodynamical solution must respect.

5 Outlook

These first experiments establish that the Light Theory Realm implementation can compute QGT-based metric and curvature at scale, drive flows that excite curvature and relax IGBP densities, and explore nontrivial two-dimensional sections of parameter space. The Reeb flow appears as a key control knob for where information density concentrates, even when static curvature is modest. Next steps:

1. Refine curvature extraction: introduce regularised scalar invariants and study their dependence on flow parameters and plaquette structure.

2. Systematic mass–geometry scans: explore alternative prime plaquette assignments, fit models relating mass, IGBP densities, and curvature invariants, and test whether any

relation survives across variations.

3. Higher-dimensional gravity probes: extend the loop scan to include more angles, phases, and Reeb couplings; look for universal geometrodynamical patterns (for example, phase transitions in ρ_{IGBP}).
4. Bulk reconstruction: use boundary QGT and IGBP data as input for a bulk metric reconstruction scheme in the Kaluza–Klein framework and compare boundary predictions from bulk geodesics to direct QGT data.

References

[1] Dimitry Jean-Noel II. Curvature metrics log. CSV log: light_theory_realm/experiments/logs/curvature_metrics_20251130_223013.csv, 2025. Baseline curvature extraction showing vanishing scalars.

[2] Dimitry Jean-Noel II. Gravity-probe parameter scan results. CSV log: light_theory_realm/experiments/logs/gravity_probe_results_20251201_004930.csv, 2025. 400-point scan over loop scale and rotation angle.

[3] Dimitry Jean-Noel II. Next-generation curvature bursts under exponential flow. CSV log: light_theory_realm/experiments/logs/nextgen_curvature_exponential_20251201_083830.csv, 2025. Per-particle curvature bursts and timing.

[4] Dimitry Jean-Noel II. Prime plaquette joint analysis. CSV table: light_theory_realm/experiments/logs/joint_analysis_20251130_223013.csv, 2025. Summary metrics per fermion.

[5] Dimitry Jean-Noel II. Prime plaquette scan dataset. CSV log: light_theory_realm/experiments/logs/plaquette_scan_20251130_222736.csv, 2025. Nine-fermion plaquette scan.